JACS
JOURNAL OF THE AMERICAN CHEMICAL SOCIETY
Article
pubs.acs.org/JACS

Highly Selective Molybdenum ONO Pincer Complex Initiates the Living Ring-Opening Metathesis Polymerization of Strained Alkynes with Exceptionally Low Polydispersity Indices

Donatela E. Bellone,[†] Justin Bours,[†] Elisabeth H. Menke,[†] and Felix R. Fischer*[,†,‡,§]

[†]Department of Chemistry, University of California Berkeley, Berkeley, California 94720, United States
[‡]Materials Sciences Division, Lawrence Berkeley National Laboratory, Berkeley, California 94720, United States
[§]Kavli Energy NanoSciences Institute at the University of California Berkeley and the Lawrence Berkeley National Laboratory, Berkeley, California 94720, United States

Supporting Information

ABSTRACT: The pseudo-octahedral molybdenum benzylidyne complex [TolC≡Mo(ONO)(OR)]·KOR (R = $CCH_3(CF_3)_2$) **1**, featuring a stabilizing ONO pincer ligand, initiates the controlled living polymerization of strained dibenzocyclooctynes at $T > 60$ °C to give high molecular weight polymers with exceptionally low polydispersities (PDI ∼ 1.02). Kinetic analyses reveal that the growing polymer chain attached to the propagating catalyst efficiently limits the rate of propagation with respect to the rate of initiation ($k_p/k_i \sim 10^{-3}$). The reversible coordination of $KOCCH_3(CF_3)_2$ to the propagating catalyst prevents undesired chain-termination and -transfer processes. The ring-opening alkyne metathesis polymerization with **1** has all the characteristics of a living polymerization and enables, for the first time, the controlled synthesis of amphiphilic block copolymers via ROAMP.

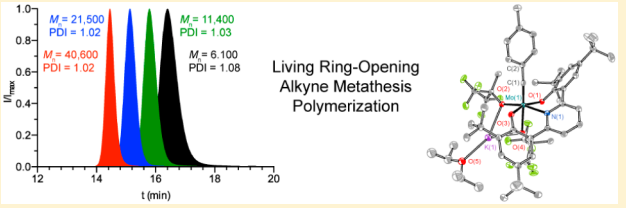

INTRODUCTION

Since its discovery in the mid-1960s, the development of stable, well-defined, and functional-group-tolerant olefin metathesis catalysts has greatly influenced the fields of organic synthesis and polymer and materials science.[1,2] Although alkene metathesis has found a wide range of applications, alkyne metathesis has only recently become the focus of attention.[3−10] Moreover, living ring-opening olefin metathesis polymerization (ROMP) has had a great impact in the areas of biomimetic synthetic polymers, self-assembled nanomaterials, and monolithic supports.[1] Despite recent synthetic advances toward highly functionalized ring-strained alkynes,[11a−d] the application of ring-opening alkyne metathesis polymerization (ROAMP) to the field of polymer synthesis has remained limited due to the lack of commercially available well-behaved catalysts.[12−17]

Presently, poly(arylene ethynylene)s, used in applications ranging from molecular photonics, electronics, to sensing, can be accessed through acyclic diyne metathesis (ADIMET) polymerization of diynes using highly active molybdenum and tungsten catalysts.[18−22] However, this step-growth process provides only very limited control over the polydispersity, length, and modality of the polymer product. Previous attempts at synthesizing polymers using ring-opening of strained alkynes showed polydispersities ranging from 1.1 to 7.0.[12,14,23] While polymers with polydispersities as low as 1.1 have been obtained, the active catalyst species is poorly defined, and the reaction requires low temperatures and rigorous air-free conditions.[15] Polymers resulting from these catalysts tend to have higher molecular weights than predicted on the basis of the monomer to catalyst loading. ^{1}H NMR experiments show that only a fraction of the catalyst is activated and contributes to the linear chain growth, indicating that the rate of propagation is larger than the rate of initiation ($k_p/k_i > 1$). The poor selectivity of alkyne metathesis catalysts for strained over unstrained alkynes in the growing polymer chain leads to significant broadening of the polydispersity index (PDI) through chain-transfer processes and "backbiting" to form cyclic structures.

In this study, we report the synthesis and the detailed mechanistic investigation of the first molecularly defined living ring-opening alkyne metathesis catalyst [TolC≡Mo(ONO)(OR)]·KOR (R = $CCH_3(CF_3)_2$, ONO = 6,6′-(pyridine-2,6-diyl)bis(2,4-di-*tert*-butylphenolate)) **1** (Figure 1). In solution, a rapid equilibrium between the -ate complex **1** and the pentacoordinate 14-electron complex **2** is observed (electron count does not include potential π-donation of electron density from alkoxide lone pairs). While the reversible association of a free alkoxide prevents undesired side reactions, the dissociation of **1** does not represent a rate-limiting step during the propagation. Kinetic studies reveal that the growing polymer chain efficiently limits the rate of propagation with respect to the rate of initiation ($k_p/k_i \sim 10^{-3}$). We herein demonstrate the outstanding control over molecular weight and polydispersity achieved in living ROAMP with **1** and the first synthesis of block copolymers through alkyne metathesis.

Received: October 23, 2014

DOI: 10.1021/ja510919v
J. Am. Chem. Soc. XXXX, XXX, XXX−XXX

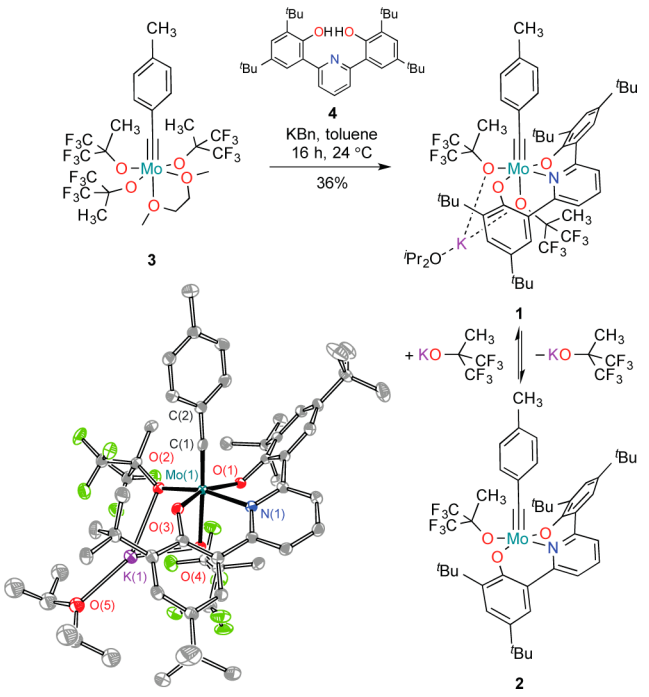

Figure 1. Synthesis of ROAMP catalyst **1**. ORTEP representation of the X-ray crystal structure of **1**. Thermal ellipsoids are drawn at the 50% probability level. Color coding: C (gray), O (red), N (blue), F (green), Mo (turquoise). Hydrogen atoms are omitted for clarity. Diisopropyl ether was refined isotropically.

RESULTS AND DISCUSSION

Catalyst **1** was synthesized through ligand exchange from the trisalkoxy molybdenum benzylidyne complex [TolC≡Mo(OR)$_3$(dme)] **3**.[24−27] While structurally related 12-electron molybdenum and tungsten complexes have been reported as catalysts for alkyne cross-metathesis and ring-closing metathesis, these highly active complexes are unsuitable for controlled ROAMP. Extensive chain transfer reactions lead to undesired broad weight distributions (PDI > 2).[6,14,28−35] In an effort to increase the selectivity of our catalyst for the activation of strained monomers over unstrained alkynes in the growing polymer chain, we incorporated a permanent electron donating, sterically demanding ONO pincer ligand **4**.[24,36a−f] This tridentate ligand stabilizes the high oxidation state of the molybdenum benzylidyne complex, prevents its dimerization in solution,[12] and irreversibly blocks one of the catalyst's active sites.[37,38] Deprotonation of the ONO pincer ligand **4** with potassium benzyl followed by addition to [TolC≡Mo(OR)$_3$(dme)] in toluene quantitatively converted **3** to the desired product **1**, by ^{1}H and ^{19}F NMR spectroscopy.

Dark brown crystals of **1** were isolated in 36% yield after recrystallization from diisopropyl ether at −35 °C. The geometry at the metal center is pseudo-octahedral. X-ray crystallography of **1** (Figure 1) confirms the presence of a C(1)≡Mo(1) triple bond with bond length of 1.760(2) Å and C(2)−C(1)−Mo(1) angle of 176.91(19)°. The tridentate ONO pincer ligand adopts a skewed conformation featuring typical Mo(1)−O(1) and Mo(1)−O(3) distances of 1.9876(16) and 2.0010(16) Å, respectively. The Mo(1)−N(1) distance of 2.2227(19) Å corresponds to a neutral L-type N−Mo bond, indicating the presence of an interaction between the lone pair of the pyridine ring and the metal center. The presence of two alkoxides and one potassium cation in the crystal structure of **1** confirms that only one alkoxide in **3** has been displaced by the ONO pincer ligand. The Mo−O distances are 2.0038(16) and 2.2475(16) Å for the hexafluoro-*tert*-butoxide *cis*, Mo(1)−O(2), and *trans*, Mo(1)−O(4), to the carbyne, respectively. The elongated Mo(1)−O(4) bond for the alkoxide *trans* to the carbyne suggests a weak interaction with an oxygen lone pair.

Crystals of **1** are stable in air for hours and can be stored for indefinite time under an atmosphere of nitrogen. In the absence of moisture and air, a solution of **1** in toluene-d_8 shows less than 5% decomposition after one month at 24 °C. In toluene-d_8, the pseudo-octahedral -ate complex **1** is in dynamic equilibrium with the dissociated pentacoordinate complex [TolC≡Mo(ONO)(OR)] (R = CCH$_3$(CF$_3$)$_2$) **2** (Supporting Information Figure S1). In THF-d_8 the alkoxide *trans* to the carbyne is replaced by the solvent, and only a single species, corresponding to a THF bound hexacoordinate complex, is observed by ^{1}H and ^{19}F NMR.

We studied the ROAMP of 3,8-dihexyloxy-5,6-dihydro-11,12-didehydrodibenzo[*a*,*e*][8]annulene (**5a**) (Scheme 1), a

Scheme 1. ROAMP of 5a,b with Catalyst 1

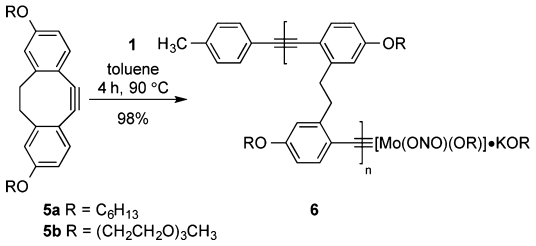

readily accessible highly solubilized ring-strained alkyne, with **1**. Addition of **1** to a solution of **5a** in toluene ([**5a**]/[**1**] = 10) at 24 °C does not lead to the formation of polymeric species within 24 h. ^{1}H and ^{19}F NMR indicate that the ROAMP catalyst **1** quantitatively initiates with a half-life of $t_{1/2}$ < 5 min with 1 equiv of **5a** to form the initiated complex **6** (n = 1) (Scheme 1). At 90 °C, however, the initiation reaction is instantaneous, and the living ROAMP of monomer **5a** (10 equiv) in toluene is completed in less than 2 h, as determined by ^{1}H NMR spectroscopy. In the absence of monomer, the molybdenum catalyst attached to the propagating polymer chain remains active and continues to incorporate equivalents of monomer added sequentially to the reaction mixture (Supporting Information Figure S2). Precipitation of the resulting polymers in MeOH affords *poly*-**5a** in greater than 90% isolated yield. GPC analysis for various monomer/catalyst loadings at 90 °C in toluene shows a PDI of ∼1.02, the lowest value ever reported for ROAMP (Figure 2, Table 1). Extended reaction times do not lead to a deterioration of the PDI. The molecular weights of *poly*-**5a** determined by GPC, calibrated to polystyrene standards, scale linearly with the conversion of monomer (Supporting Information Figure S2), are proportional to the initial [**5a**]/[**1**] loading, and show a unimodal distribution (Figure 2). No evidence for branching or the formation of cyclic polymers could be observed by ^{1}H NMR analysis and mass spectrometry (Supporting Information Figure S3). ^{1}H NMR end-group analysis of the tolyl group reveals that GPC overestimates the M_n of *poly*-**5a**. A correction factor ∼0.7−1.0 correlates well with the degree of polymerization determined by NMR analysis and the expected molecular weight based on the [**5a**]/[**1**] loading.

DOI: 10.1021/ja510919v
J. Am. Chem. Soc. XXXX, XXX, XXX−XXX

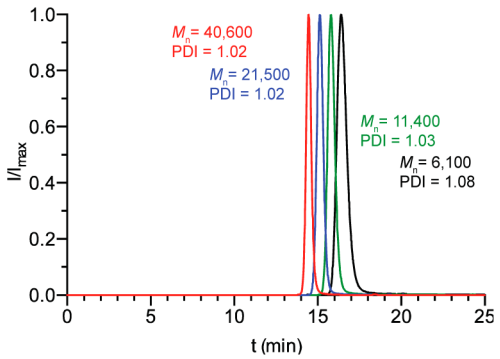

Figure 2. GPC traces for *poly*-**5a** produced through ROAMP of **5a** with catalyst **1** at variable loadings of [**5a**]/[**1**] = 100 (red), 50 (blue), 20 (green), 10 (black) (T = 90°), calibrated to polystyrene standards.

Table 1. Molecular Weight Analysis of *poly*-5a

[**5a**]/[**1**]	T (°C)	M_n theory	M_n GPC[a]	M_w GPC[a]	X_n[b]	PDI GPC[a]
10/1	60	4000	7200	7700		1.07
10/1	70	4000	7300	7800		1.07
10/1	80	4000	9100	9500		1.04
10/1	90	4000	6100	6600	11	1.08
20/1	90	8100	11 400	11 800	23	1.03
50/1	90	20 200	21 500	22 100	47	1.02
100/1	90	40 400	40 600	41 500	99	1.02

[a]Calibrated to narrow polydispersity polystyrene standards. [b]Degree of polymerization determined by ^{1}H NMR end-group analysis.

The proposed kinetic scheme for the polymerization of a ring-strained monomer **5a** with catalyst **1** is depicted in Scheme 2. In a fast initiation reaction, 1 equiv of **5a** reacts with **2** to

Scheme 2. Kinetic Scheme for the ROAMP of 5a

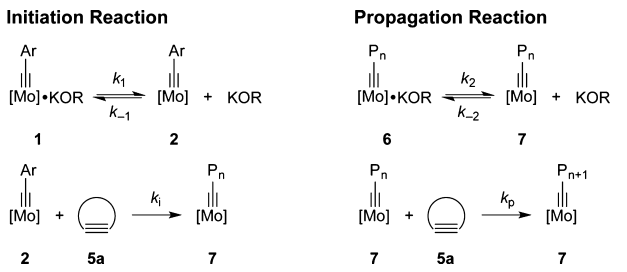

form the initiated complex **7** (n = 1). Binding of KOR to **7** stabilizes the initiated complex and reversibly blocks the active site. Dissociation of KOR from **6** regenerates the active propagating species that undergoes linear chain-growth polymerization with further equivalents of **5a** to form extended living polymer chains.

To meet the stringent criteria for a living polymerization the initiation of the catalyst must be fast and quantitative ($k_i > k_p$), the concentration of propagating species has to remain constant throughout the reaction, all propagating chains have to grow at the same rate, and irreversible termination and chain-transfer processes should be absent.[39a,b] The rate laws for both the initiation and the propagation reaction are derived employing the following assumptions: (i) The release of ring-strain stored in the cyclic monomer **5a** makes the initiation and the propagation irreversible. (ii) The rate of propagation k_p is comparable for all propagating species irrespective of the degree of polymerization. (iii) The dissociation equilibria are faster than the rate of initiation/propagation. (iv) Catalyst **1** initiates quantitatively. It is thus reasonable to assume that, during the polymerization, the concentration of **7** reaches steady state. The resulting rate law for the polymerization is

$$-\frac{d[M]}{dt} = \frac{k_p[C]_0[M]}{\left(\frac{[KOR]}{K_{diss,p}} + 1\right)} = k_{p,obs}[C]_0[M] \quad (1)$$

where [M] is the concentration of monomer **5a**, $[C]_0$ is the starting concentration of **1**, and $K_{diss,p}$ is the dissociation constant of **6**. Since the rate of initiation of complex **2** is very fast at the temperatures used throughout the polymerization, we herein rely on an approximation based on initial rates of reaction

$$\frac{d[C_i]}{dt} = \frac{k_i[C]_0[M]}{\left(\frac{[KOR]}{K_{diss}} + 1\right)} = k_{i,obs}[C]_0[M] \quad (2)$$

where $[C_i]$ is the concentration of all initiated species **6**/**7**, and K_{diss} is the dissociation constant of **1**.

Experimental data are consistent with the proposed rate laws. Plots of $\ln([M]/[M]_0)$ over time (Figure 3) are linear

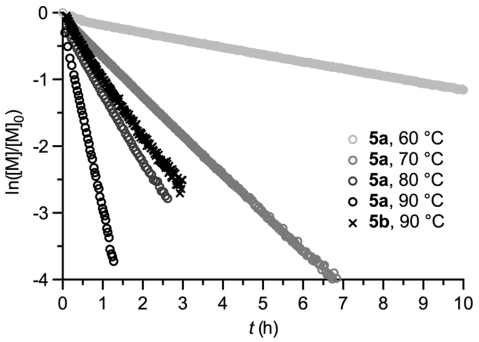

Figure 3. Kinetic studies of the rate of polymerization of **5a** and **5b** by **1** at various temperatures.

throughout the entire polymerization and fit a rate law first order in monomer. The concentration of propagating species is constant throughout the reaction, and irreversible termination processes are absent. The observed rate of propagation shows a linear dependence on the catalyst loading (Supporting Information Figure S4). A plot of $1/([KOR]/K_{diss,p}+1)$ versus $k_{p,obs}$ at 90 °C shows a linear correlation between the rate of propagation and the inverse of the concentration of KOR (Supporting Information Figure S5). Similarly, the rate of initiation shows a linear dependence on the concentration of monomer [M] and catalyst $[C]_0$. Excess KOR added to the reaction mixture slows the rate of initiation. The observed rate constants $k_{i,obs}$ and $k_{p,obs}$ at various temperatures are summarized in Table 2. The standard activation enthalpy for the initiation ($\Delta H^{\ddagger}$ = 20.7 ± 1.2 kcal mol^{-1}) and for the propagation reaction ($\Delta H^{\ddagger}$ = 23.0 ± 1.2 kcal mol^{-1}) can be derived from Eyring analysis (Supporting Information Figures S6–S7).

From Eyring analysis we conclude that, for the polymerization of **5a** with catalyst **1** at 90 °C, the rate of initiation is ~10^3 times faster than the rate of propagation. Quantitative initiation of catalyst **1** is practically instantaneous upon addition to a solution of the monomer. All propagating species

DOI: 10.1021/ja510919v
J. Am. Chem. Soc. XXXX, XXX, XXX−XXX

Table 2. Observed Rates of Initiation $k_{obs,i}$ and Rates of Propagation $k_{obs,p}$ at Different Temperatures

T (°C)	$k_{i,obs}$ (M^{-1} s^{-1})[a]	T (°C)	$k_{p,obs}$ (M^{-1} s^{-1})
10	0.0158	60	0.0227
15	0.0407	70	0.0787
20	0.1210	80	0.1642
25	0.2197	90	0.5271
30	0.4066		
35	0.8650		

[a]The rate of initiation at T > 40 °C is too fast to be monitored by ^{19}F NMR.

incorporate monomer **5a** at comparable rates (k_p) to give polymers with exceptionally narrow weight distributions.

We studied the role of the weakly coordinating alkoxide ligand during the initiation and the polymerization reaction. At elevated temperatures (T > 60 °C) a rapid equilibrium is established between the -ate complexes **1** and **6**, and the dissociated complexes **2** and **7**, respectively (Supporting Information Figure S1). The dissociation constants of **1** (K_{diss}) and **6** ($K_{diss,p}$) at selected temperatures are summarized in Table 3. Van't Hoff analysis reveals that the changes in

Table 3. Dissociation Constants (K_{diss}, $K_{p,diss}$) and Selected Rate Constants (k_1, k_2) for 1 and 6 at Different Temperatures

T (°C)	K_{diss} (M)	k_1 (s^{-1})	T (°C)	$K_{p,diss}$ (M)	k_2 (s^{-1})
30	0.78×10^{-3}	7.9	10.0	3.70×10^{-3}	1.2
40	1.22×10^{-3}	15.1	15.0	4.26×10^{-3}	1.9
50	1.98×10^{-3}	27.7	20.0	5.98×10^{-3}	2.9
60	3.40×10^{-3}	43.2	25.0	6.62×10^{-3}	4.3
70	4.66×10^{-3}	*a*	27.5	7.13×10^{-3}	4.9
80	6.84×10^{-3}	*a*	30.0	8.07×10^{-3}	6.4
			32.5	9.00×10^{-3}	7.1
			35.0	9.94×10^{-3}	8.2

[a]The resonance signals in the ^{19}F NMR are broadened and could not be inverted for SIR experiments.

standard free enthalpy ($\Delta H°$ = 7.1 ± 0.2 kcal mol^{-1}) and entropy ($\Delta S°$ = 13.8 ± 0.6 eu) associated with the dissociation of KOR from **6** are smaller than the respective changes observed for the dissociation of **1** ($\Delta H°$ = 9.5 ± 0.5 kcal mol^{-1}, $\Delta S°$ = 16.8 ± 2.1 eu) (Supporting Information Figures S8–S9). The rates of dissociation (k_1 and k_2) at various temperatures were measured by selective inversion recovery (SIR) ^{19}F NMR experiments (Table 3, Supporting Information Figures S10–S12).[40,41] The standard activation enthalpies for the dissociation of **1** ($\Delta H^{‡}$ = 10.4 ± 0.6 kcal mol^{-1}) and **6** ($\Delta H^{‡}$ = 12.8 ± 0.4 kcal mol^{-1}) were derived from Eyring plots (Supporting Information Figures S13–S14). To highlight the importance of the KOR dissociation equilibrium for the performance of ROAMP catalyst **1**, we polymerized **5a** in the presence of varying amounts of a Lewis acid. Addition of 2 equiv of BPh_3 to a solution of **1** in toluene efficiently shifts the dissociation equilibrium toward the pentacoordiante complex **2** (2 equiv of a Lewis acid are required to trap the labile hexafluoro-*tert*-butoxide and the isopropyl ether found in the crystal unit cell of **1**). Polymers formed in the absence of free hexafluoro-*tert*-butoxide feature broad weight distributions (PDI > 1.3) and M_n values that do not reflect the initial [**5a**]/[**1**] loading (Supporting Information Figure S15).

Figure 4 summarizes the experimentally determined kinetic and thermodynamic parameters for the initiation and the

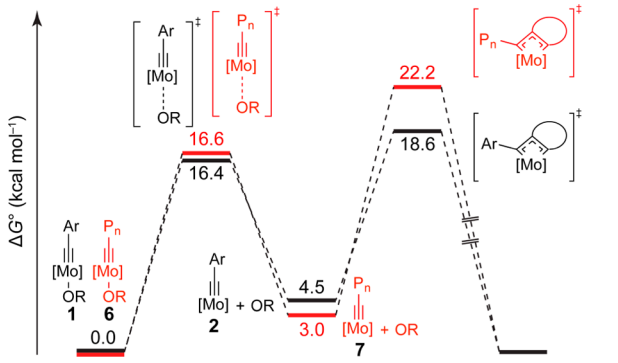

Figure 4. Reaction coordinate diagram for the initiation (black) and the propagation reaction (red) at 25 °C.

propagation reaction at standard conditions. The association of KOR is a fast pre-equilibrium to the rate-determining step. The rate of initiation is faster than the rate of propagation even though the equilibrium concentration of **2** is lower than the concentration of the propagating species **7**. The rate-determining transition state for the propagation is 3.6 kcal mol^{-1} higher than the transition state for the initiation reaction. The observed difference in metathesis activity between **2** and **7** can be rationalized by a combination of electronic and steric effects imposed by the growing polymer chain. The steric bulk associated with the *ortho*-substituted polymer backbone increases the barrier for the incorporation of the next ring-strained monomer. The initiated catalyst **7** features an electron donating hexyloxy substituent on the benzylidyne that further stabilizes the Mo(VI) complex as compared to the CH_3 group in **2** (Scheme 1).

To expand the substrate scope of ROAMP with catalyst **1** we synthesized ring-strained monomer **5b** (Scheme 1) featuring solubilizing triethylene glylcol chains. Even though the ether oxygen atoms in the side chains compete with the free alkoxide and the ring strained monomer for binding to the propagating molybdenum species **7**, the M_n and the PDIs for polymers obtained from the ring opening of **5b** are comparable to **5a** and are summarized in Table 4. The observed rate constant for the ROAMP of **5b** at 90 °C is slower ($k_{p,obs}$ = 0.144 M^{-1} s^{-1}) than for **5a** resulting in a $t_{1/2}$ ~ 38 min (Figure 3).

With two chemically distinct monomers at hand we studied the performance of ROAMP catalyst **1** in the synthesis of amphiphilic block copolymers. At 90 °C, 10 (20) equiv of **5a** were reacted with **1** for 30 min. Prior to the addition of 10 (20) equiv of **5b**, an aliquot was removed from the reaction mixture and analyzed by GPC. After the consumption of all monomers, as judged by ^1H NMR spectroscopy, the reaction was quenched with MeOH. Unlike *poly*-**5a**, low molecular weight (M_n = 8000) *poly*-**5a**-*block*-*poly*-**5b** is soluble in MeOH and only precipitates from concentrated solutions as a pale orange solid in >90% yield. GPC analysis reveals an increase in M_n upon addition of **5b** to the living chains of *poly*-**5a** (Supporting Information Figure S16). The PDI of *poly*-**5a**-*block*-*poly*-**5b** is exceptionally low (1.08) and matches the catalyst performance achieved for the respective homopolymers. End-group analysis reveals that the ratio of monomers in *poly*-**5a**-*block*-*poly*-**5b** scales linearly with the monomer loading.

DOI: 10.1021/ja510919v
J. Am. Chem. Soc. XXXX, XXX, XXX–XXX

Table 4. Molecular Weight Analysis of *poly*-5b and Block Copolymers *poly*-5a-block-*poly*-5b

[5a]/[5b]/[1]	T (°C)	M_n theory	M_n GPC[a]	M_w GPC[a]	$X_{n[5a]}/X_{n[5b]}$[b]	PDI GPC[a]
0/10/1	90	5400	5700	6100	0/9	1.08
10/0/1[c]	90	4000	3300	3800	10/0	1.15
10/10/1	90	8300	11 000	11 800	11/12	1.07
20/0/1[c]	90	8100	14 400	15 000	20/0	1.04
20/20/1	90	13 400	25 400	27 200	20/20	1.07

[a]Calibrated to narrow polydispersity polystyrene standards. [b]Degree of polymerization determined by ^{1}H NMR end-group analysis. [c]Sample taken from the reaction mixture after t = 30 min.

CONCLUSION

In summary, we have described the synthesis of the first molecularly well-defined 16-electron ROAMP catalyst based on a molybdenum benzylidyne ONO pincer complex [TolC≡Mo(ONO)(OR)]·KOR (R = $CCH_3(CF_3)_2$) **1**. The incorporation of a permanent electron donating tridentate ligand irreversibly blocks one of the catalyst's active sites, prevents undesired alkyne polymerization reactions, and significantly increases its stability toward air and moisture. The catalyst is capable of selectively ring-opening strained alkynes in a controlled polymerization to yield high molecular weight polymers with exceptionally low PDIs (1.02). Mechanistic studies reveal that the ROAMP catalyst **1** meets all the criteria for a controlled living polymerization: the initiation reaction is quantitative and ~10^3 times faster than the propagation ($k_i > k_p$), the concentration of catalytically active complex is constant throughout the reaction, and all propagating chains grow at the same rate. The reversible coordination of KOR to the propagating catalyst prevents undesired chain termination and bimolecular decomposition of the catalyst. We demonstrate for the first time the synthesis of structurally well-defined block copolymers through a controlled living ROAMP. The catalyst developed herein provides an unprecedented control and access to functionalized homo- and block copolymers derived from ring-strained alkynes with potential applications in advanced thin-film electronics/photonics, molecular sensing, and nanopatterning.

EXPERIMENTAL SECTION

Materials and General Methods. Unless otherwise stated, all manipulations of air and/or moisture sensitive compounds were performed in oven-dried glassware, under an atmosphere of Ar or N_2. Solvents were dried by passing through a column of alumina and were degassed by vigorous bubbling of N_2 or Ar through the solvent for 20 min. All ^{1}H, {^{1}H}^{13}C, and ^{19}F NMR spectra were recorded on Bruker AV-600, DRX-500, AV-500, and AV-900 MHz spectrometers, and are referenced to residual solvent peaks ($CDCl_3$ ^{1}H NMR δ = 7.26 ppm, ^{13}C NMR δ = 77.16 ppm; C_6D_6 ^{1}H NMR δ = 7.16 ppm, ^{13}C NMR δ = 128.06 ppm; Tol-d_8 ^{1}H NMR δ = 2.08 ppm; THF-d_8 ^{1}H NMR δ = 1.78 ppm, ^{13}C NMR δ = 67.21 ppm) or trifluorotoluene (^{19}F NMR δ = −63.72 ppm). The concentrations of **1**, **2**, **6**, **7**, and $KOCCH_3(CF_3)_2$ were determined by ^{19}F NMR using the ERETIC method against an external standard of 13.6 mM trifluorotoluene in Tol-d_8.[42] The concentration of monomer **5a,b** was verified by ^{1}H NMR applying the ERETIC method against an external standard of 19.4 mM of hexamethyldisiloxane in Tol-d_8.[41] Selective inversion recovery (SIR) experiments were performed using TopSpin for data acquisition, and fitted with CIFIT.[40,41] The temperature in all VT NMR experiments is calibrated to ethylene glycol or MeOH standards. ESI mass spectrometry was performed on a Finnigan LTQFT (Thermo) spectrometer in positive ionization mode. MALDI mass spectrometry was performed on a Voyager-DE PRO (Applied Biosystems Voyager System 6322) in positive mode using a matrix of dithranol. Elemental analysis (CHN) was performed on a PerkinElmer 2400 Series II combustion analyzer (values are given in %). Gel permeation chromatography (GPC) was carried out on a LC/MS Agilent 1260 Infinity set up with a guard and two Agilent Polypore 300 mm × 7.5 mm columns at 35 °C and calibrated to narrow polydispersity polystyrene standards ranging from M_w = 100 to 4 068 981. X-ray crystallography was performed on APEX II QUAZAR, using a Microfocus Sealed Source (Incoatec IμS; Mo Kα radiation), Kappa Geometry with DX (Bruker-AXS build) goniostat, a Bruker APEX II detector, QUAZAR multilayer mirrors as the radiation monochromator, and Oxford Cryostream 700 for **1**. Crystallographic data were refined with SHELXL-97, solved with SIR-2007, visualized with ORTEP-32, and finalized with WinGX. **4**,[24] and KBn[43] were synthesized following literature procedures.

Preparation of [TolC≡Mo(ONO)(OCCH$_3$(CF$_3$)$_2$)]·KOCCH$_3$(CF$_3$)$_2$·^{i}Pr$_2$O (1). A 25 mL vial was charged with **4** (88 mg, 0.18 mmol, 1.0 equiv) in dry toluene (3 mL). A suspension of KBn (48 mg, 0.37 mmol 2.05 equiv) in dry toluene (8 mL) was added dropwise and the reaction mixture stirred for 15 min at 24 °C. The resulting suspension was added dropwise to a solution of **3** (164 mg, 0.2 mmol, 1.1 equiv) in toluene (7 mL). An immediate color change to dark brown was observed, and the reaction mixture was stirred for 30 h at 24 °C. The suspension was filtered, and the solvent was removed under dynamic vacuum. The precipitate was dissolved in cold CH_2Cl_2/pentane (3:2, 4 mL) and filtered through a precooled frit. ^{i}Pr$_2$O (1 mL) was added to the solution, and the solvent was removed under vacuum. The residue was recrystallized from ^{i}Pr$_2$O (2 mL) (−35 °C), to yield pure **1** (78 mg, 36%) as a dark brown crystalline solid. Crystals for X-ray analysis were grown from saturated ^{i}Pr$_2$O solutions at −35 °C. In toluene, **1** is in equilibrium with the dissociated pentacoordinate complex **2** and free $KOC(CF_3)_2CH_3$. ^{1}H NMR (500 MHz, Tol-d_8, 22 °C) δ = 7.70 (**2**), 7.63 (s, 2H, Ar-*H*), 7.42 (s, 2H, Ar-*H*), 7.27 (**2**), 7.20 (d, J = 8.0 Hz, 2H, 3,5-NC_5H_2H), 6.91 (t, J = 8.0 Hz, 1H, 4-NC_5H_2H), 6.58 (d, J = 7.6 Hz, 2H, C_6H_2 H_2CH_3), 6.44 (**2**), 6.30 (d, J = 7.6 Hz, 2H, $C_6H_2H_2CH_3$), 6.26 (**2**), 2.01 (s, 3H, C_6H_4−CH_3), 1.93 (s, 3H, $OC(CF_3)_2CH_3$), 1.71 (**2**), 1.64 (s, 18H, ^{t}Bu-*H*), 1.46 (s, 18H, ^{t}Bu-*H*), 1.37 (**2**), 1.00 (s, 3H, K-$OC(CF_3)_2CH_3$) ppm. ^{19}F NMR (470 MHz, Tol-d_8, 22 °C) δ = −76.79 (**2**), −77.80, −78.26, −81.18 (dissociated $KOC(CF_3)_2CH_3$) ppm. In THF, only the dissociated species **2**·THF is observed, resulting in the presence of free $KOC(CF_3)_2CH_3$. ^{1}H NMR (500 MHz, THF-d_8, 22 °C) δ = 7.92 (t, J = 8.0 Hz, 1H, 4-NC_5H_2H), 7.70 (d, J = 8.0 Hz, 2H, 3,5-NC_5H_2H), 7.52 (d, J = 2.3 Hz, 2H, Ar-*H*), 7.46 (d, J = 2.3 Hz, 2H, Ar-*H*), 6.74 (d, J = 7.9 Hz, 2H, C_6H_2 H_2CH_3), 6.12 (d, J = 7.9 Hz, 2H, $C_6H_2H_2CH_3$), 2.20 (s, 3H, $C_6H_4CH_3$), 1.78 (s, 3H, $OC(CF_3)_2CH_3$), 1.52 (s, 18H, ^{t}Bu-*H*), 1.39 (s, 18H, ^{t}Bu-*H*) ppm. {^{1}H}^{13}C NMR (126 MHz, THF-d_8, 22 °C) δ = 307.5, 166.2, 155.6, 141.5, 140.5, 139.1, 138.8, 137.5, 136.8, 130.3, 127.6, 126.0, 125.4, 124.9, 123.1, 84.2, 36.0, 34.8, 32.4, 30.8, 23.5, 21.6 ppm. ^{19}F NMR (470 MHz, THF-d_8, 22 °C) δ = −76.92 ppm. FTMS (ESI-TOF) (m/z): [[TolC≡Mo(ONO)(OCCH$_3$(CF$_3$)$_2$)] + H]$^+$ calcd [$C_{45}H_{54}F_6MoNO_3$], 868.3056; found 868.3076. Anal. Calcd for [[TolC≡Mo(ONO)(OCCH$_3$(CF$_3$)$_2$)$_2$]KO^{i}Pr$_2$]$_2$·^{i}Pr$_2$O: C, 56.21; H, 6.26; N, 1.13. Found: C, 56.04; H, 6.40; N, 1.38. Crystal data: CCDC no., 998197; formula, $C_{60.5}H_{83}F_{12}KMoNO_{6.25}$; fw, 1297.32 g mol^{-1}; temp, 100(2) K; cryst syst, monoclinic; space group, $P2_1/n$; color, black; a, 12.751(5) Å; b, 29.140(5) Å; c, 17.008(5) Å; α, 90.000(5)°; β, 93.406(5)°; γ, 90.000(5)°; V, 6308(3) Å^3; Z, 4; R1, 0.0367; wR2, 0.0818; GOF, 1.051.

DOI: 10.1021/ja510919v
J. Am. Chem. Soc. XXXX, XXX, XXX−XXX

Preparation of *poly*-3,8-Dihexyloxy-5,6-dihydro-11,12-didehydrodibenzo[*a*,*e*][8]annulene (*poly*-5a). A 10 mL resealable Schlenk tube was charged with a stock solution of **5a** (220 mM) in toluene. If required, the solution was diluted with additional dry toluene to reach a total of 0.5 mL. A stock solution of **1** (11 mM, 100 μL) in toluene was added, and the reaction mixture was heated in a bath at 90 °C for 2 h. The reaction mixture was cooled, and polymers were precipitated with MeOH (2 mL). The precipitate was filtered, washed with MeOH (2 mL), and dried in vacuum to yield *poly*-**5a** (92% isolated yield) as a pale brown solid. ^{1}H NMR (600 MHz, $CDCl_3$, 22 °C) δ = 7.40 (d, J = 8.4 Hz, 2H, Ar-*H*), 6.77−6.52 (m, 4H, Ar-*H*), 3.67 (t, J = 6.5 Hz, 4H, OCH_2), 3.19 (s, 4H, CH_2), 1.69−1.58 (m, 4H, $O(CH_2)_5CH_3$), 1.41−1.19 (m, 12H, $O(CH_2)_5CH_3$), 0.87 (t, J = 7.0 Hz, 6H, CH_3) ppm. $\{^1H\}^{13}C$ NMR (151 MHz, $CDCl_3$, 22 °C) δ = 159.2, 145.3, 133.5, 115.3, 114.6, 113.0, 90.5, 67.9, 36.6, 31.8, 29.4, 25.9, 22.8, 14.2 ppm.

Preparation of *poly*-3,8-Di-(2-(2-(2-methoxyethoxy)ethoxy)-ethoxy)-5,6-dihydro-11,12-didehydrodibenzo[*a*,*e*][8]annulene (*poly*-5b). A 10 mL resealable Schlenk tube was charged with a stock solution of **5b** (220 mM) in toluene. If required, the solution was diluted with additional dry toluene to reach a total of 0.5 mL. A stock solution of **1** (11 mM, 100 μL) in toluene was added, and the reaction mixture was heated in a bath at 90 °C for 7 h. The reaction mixture was concentrated and the solid residue suspended in cold MeOH (2 mL). The precipitate was filtered, washed with cold MeOH (2 mL), and dried in vacuum to yield *poly*-**5b** (53% isolated yield) as a pale orange solid. ^{1}H NMR (900 MHz, $CDCl_3$, 22 °C) δ = 7.38 (s, 2H, Ar−H), 6.66 (s, 4H, Ar−H), 3.91−3.24 (m, 30H), 3.17 (s, 4H, CH_2) ppm. $\{^1H\}^{13}C$ NMR (226 MHz, $CDCl_3$, 22 °C) δ = 158.8, 145.1, 133.6, 115.7, 114.8, 113.1, 90.6, 72.0, 70.9, 70.7 (2C), 69.7, 67.4, 59.2, 36.2 ppm.

Preparation of *poly*-5a-block-*poly*-5b. A 10 mL resealable Schlenk tube was charged with a stock solution of **5a** (230 mM, 200 μL) in toluene. A stock solution of **1** (7.7 mM, 300 μL) in toluene was added, and the reaction mixture was heated at 90 °C for 30 min. An aliquot (150 μL) was quickly removed and precipitated with MeOH (2 mL). A stock solution of **5b** (46 mM, 700 μL) in toluene was added, and the reaction was heated for an additional 7 h. The reaction mixture was cooled, and polymers were precipitated with MeOH (2 mL). The precipitate was filtered, washed with MeOH (2 mL), and dried in vacuum to yield *poly*-**5a**-block-*poly*-**5b** (94% isolated yield) as a pale orange solid. ^{1}H NMR (500 MHz, $CDCl_3$, 22 °C) δ = 7.40 (d, J = 8.4 Hz, 4H, Ar-*H*), 6.79−6.42 (m, 8H, Ar-*H*), 4.19−3.42 (m, 34H), 3.18 (s, 8H, CH_2), 1.79−1.49 (m, 4H, $O(CH_2)_5CH_3$), 1.40−1.16 (m, 12H, $O(CH_2)_5CH_3$), 0.86 (t, J = 6.9 Hz, 6H, CH_3) ppm. $\{^1H\}^{13}C$ NMR (126 MHz, $CDCl_3$, 22 °C) δ = 159.2, 145.2, 133.4, 115.2, 114.5, 113.0, 90.4, 72.0, 70.9, 70.7 (2C), 69.7 (2C), 67.9, 59.2, 36.6, 31.8, 29.4, 25.9, 22.8, 14.2 ppm.

■ ASSOCIATED CONTENT

Ⓢ Supporting Information

Figures S1−S16; methods and instrumentation; synthetic procedures for **3**, **5a**, and **5b** and characterization; kinetic experiments; ligand dissociation studies; NMR spectra (Figures S17−S31); and X-ray crystallographic data (Tables S1−S10 and CIF). This material is available free of charge via the Internet at http://pubs.acs.org.

■ AUTHOR INFORMATION

Corresponding Author

ffischer@berkeley.edu

Notes

The authors declare no competing financial interest.

■ ACKNOWLEDGMENTS

Research was supported by the Donors of the American Chemical Society Petroleum Research Fund under Contract 52722-DNI7, Berkeley NMR Facility is supported in part by NIH Grant SRR023679A, and X-ray Facility is supported in part by NIH Shared Instrumentation Grant S10-RR027172. D.E.B. acknowledges fellowship support through the Abrahamson Foundation, E.H.M. acknowledges fellowship support through the German Academic Exchange Service (DAAD). The authors acknowledge Prof. Alex D. Bain for helpful discussions relating to the SIR experiments, Dr. Christian Canlas for support with NMR acquisition, Dr. Antonio DiPasquale for assistance with X-ray analysis, and Dr. Rita Nichiporuk for assistance with mass spectrometry.

■ REFERENCES

(1) *Handbook of Metathesis*; Grubbs, R. H., Ed.; Wiley-VCH: Weinheim, 2003; Vol. *1*−*3*.
(2) Schrock, R. R. *Angew. Chem., Int. Ed.* **2006**, *45*, 3748−3759.
(3) Fürstner, A. *Angew. Chem., Int. Ed.* **2013**, *52*, 2794−2819.
(4) Schrock, R. R. *Chem. Commun.* **2013**, *49*, 5529−5531.
(5) Jyothish, K.; Zhang, W. *Angew. Chem., Int. Ed.* **2011**, *50*, 8628−8630.
(6) Wu, X.; Tamm, M. *Beilstein J. Org. Chem.* **2011**, *7*, 82−93.
(7) Tamm, M. *Chim. Oggi* **2010**, *28*, 60−63.
(8) Zhang, W.; Moore, J. S. *Adv. Synth. Catal.* **2007**, *349*, 93−120.
(9) Fürstner, A.; Davies, P. W. *Chem. Commun.* **2005**, 2307−2320.
(10) Schrock, R. R. *Chem. Rev.* **2002**, *102*, 145−179.
(11) (a) Poloukhtine, A. A.; Mbua, N. E.; Wolfert, M. A.; Boons, G.; Popik, V. V. *J. Am. Chem. Soc.* **2009**, *131*, 15769−15776. (b) Jewett, J. C.; Sletten, E. M.; Bertozzi, C. R. *J. Am. Chem. Soc.* **2010**, *132*, 3688−3690. (c) Friscount, F.; Ledin, P. A.; Mbua, N. E.; Flanagan-Steet, H. R.; Wolfert, M. A.; Steet, R.; Boons, G. *J. Am. Chem. Soc.* **2012**, *134*, 5381−5389. (d) Arumugam, S. A.; Popik, V. V. J. *Org. Chem.* **2014**, *79*, 2702−2708.
(12) Paley, D. W.; Sedbrook, D. F.; Decatur, J.; Fischer, F. R.; Steigerwald, M. L.; Nuckolls, C. *Angew. Chem., Int. Ed.* **2013**, *52*, 4591−4594.
(13) Sedbrook, D. F.; Paley, D. W.; Steigerwald, M. L.; Nuckolls, C.; Fischer, F. R. *Macromolecules* **2012**, *45*, 5040−5044.
(14) Lysenko, S.; Haberlag, B.; Wu, X.; Tamm, M. *Macromol. Symp.* **2010**, *293*, 20−23.
(15) Fischer, F. R.; Nuckolls, C. *Angew. Chem., Int. Ed.* **2010**, *49*, 7257−7260.
(16) Zhang, X. P.; Bazan, G. C. *Macromolecules* **1994**, *27*, 4627−4628.
(17) Krouse, S.; Schrock, R.; Cohen, R. *Macromolecules* **1987**, *20*, 903−904.
(18) Bunz, U. H. F. *Acc. Chem. Res.* **2001**, *34*, 998−1010.
(19) McQuade, D. T.; Pullen, A. E.; Swager, T. M. *Chem. Rev.* **2000**, *100*, 2537.
(20) Voskerician, G.; Weder, C. *Adv. Polym. Sci.* **2005**, *177*, 209−248.
(21) Zhang, W.; Moore, J. S. *Macromolecules* **2004**, *37*, 3973−3975.
(22) Blankenburg, L.; Bunz, U. H. F.; Klemm, E.; Moore, J. S.; Pautzsch, T.; Ray, C. R.; Swager, T. M.; Voskerician, G.; Weder, C.; Yamaguchi, I.; Yamamoto, T.; Yasuda, T.; Zheng, J. *Poly(arylene ethynylene)s: From Synthesis to Application*; Weder, C., Ed.; Springer: Berlin, 2005.
(23) Krouse, S.; Schrock, R. *Macromolecules* **1989**, *22*, 2569−2576.
(24) Fu, R.; Bercaw, J. E.; Labinger, J. A. *Organometallics.* **2011**, *30*, 6751−6765.
(25) Fischer, E. O.; Massböl, A. *Chem. Ber.* **1967**, *100*, 2445−2456.
(26) Fischer, E. O.; Kreis, G.; Kreiter, C. G.; Müller, J.; Huttner, G.; Lorenz, H. *Angew. Chem., Int. Ed. Engl.* **1973**, *12*, 564−565.
(27) Haberlag, B.; Wu, X.; Brandhorst, K.; Grunenberg, J.; Daniliuc, C. G.; Jones, P. G.; Tamm, M. *Chem.—Eur. J.* **2010**, *16*, 8868−8877.
(28) Freudenberger, J. H.; Schrock, R. R.; Churchill, M. R.; Rheingold, A. L.; Ziller, J. W. *Organometallics* **1984**, *3*, 1563−1573.
(29) McCullough, L. G.; Schrock, R. R. *J. Am. Chem. Soc.* **1984**, *106*, 4067−4068.

DOI: 10.1021/ja510919v
J. Am. Chem. Soc. XXXX, XXX, XXX−XXX

(30) McCullough, L. G.; Schrock, R. R.; Dewan, J. C. *J. Am. Chem. Soc.* **1985**, *107*, 5987−5998.
(31) Beer, S.; Hrib, C. G.; Jones, P. G.; Brandhorst, K.; Grunenberg, J.; Tamm, M. *Angew. Chem., Int. Ed.* **2007**, *46*, 8890−8894.
(32) Beer, S.; Brandhorst, K.; Hrib, C. G.; Wu, X.; Haberlag, B.; Grunenberg, J.; Jones, P. G.; Tamm, M. *Organometallics* **2009**, *28*, 1534−1545.
(33) Wu, X.; Daniliuc, C. G.; Hrib, C. G.; Tamm, M. *J. Organomet. Chem.* **2011**, *696*, 4147−4151.
(34) Haberlag, B.; Freytag, M.; Daniliuc, C. G.; Jones, P. G.; Tamm, M. *Angew. Chem., Int. Ed.* **2012**, *51*, 13019−13022.
(35) Lysenko, S.; Daniliuc, C. G.; Jones, P. G.; Tamm, M. *J. Organomet. Chem.* **2013**, *744*, 7−14.
(36) (a) O'Reilly, M. E.; Veige, A. S. *Chem. Soc. Rev.* **2014**, *43*, 6325−6369. (b) O'Reilly, M. E.; Nadif, S. S.; Ghiviriga, I.; Abboud, K. A.; Veige, A. S. *Organometallics* **2014**, *33*, 836−839. (c) O'Reilly, M. E.; Ghiviriga, I.; Abboud, K. A.; Veige, A. S. *Dalton Trans.* **2013**, *42*, 3326−3336. (d) McGowan, K. P.; O'Reilly, M. E.; Ghiviriga, I.; Abboud, K. A.; Veige, A. S. *Chem. Sci.* **2013**, *4*, 1145−1155. (e) O'Reilly, M. E.; Ghiviriga, I.; Abboud, K. A.; Veige, A. S. *J. Am. Chem. Soc.* **2012**, *134*, 11185−11195. (f) Sakar, S.; McGowan, K. P.; Kuppuswamy, S.; Ghiviriga, I.; Abboud, K. A.; Veige, A. S. *J. Am. Chem. Soc.* **2012**, *134*, 4509−4512.
(37) Wu, Z.; Wheeler, D. R.; Grubbs, R. H. *J. Am. Chem. Soc.* **1992**, *114*, 146−151.
(38) Bielawski, C. W.; Grubbs, R. H. *Prog. Polym. Sci.* **2007**, *32*, 1−29.
(39) (a) Matyjaszewski, K. *J. Phys. Org. Chem.* **1995**, *8*, 197−207. (b) Flory, P. J. *J. Am. Chem. Soc.* **1940**, *62*, 1561.
(40) Bain, A. D.; Cramer, J. A. *J. Magn. Reson., Ser. A* **1996**, *118*, 21−27.
(41) Bain, A. D. *Prog. Nucl. Magn. Reson. Spectrosc.* **2003**, *43*, 63−103.
(42) Akoka, S.; Barantin, L.; Trierweiler, M. *Anal. Chem.* **1999**, *71*, 2554−2557.
(43) Schlosser, M.; Hartman, R. *Angew. Chem., Int. Ed.* **1973**, *12*, 508−509.

DOI: 10.1021/ja510919v
J. Am. Chem. Soc. XXXX, XXX, XXX−XXX